

Simulation of f -Mode Propagation Through a Cluster of Small Identical Magnetic Flux Tubes

Solar Physics

K. Daïffallah¹

© Springer ●●●

Abstract Motivated by the question of how to distinguish seismically between monolithic and cluster models of sunspots, we have simulated the propagation of an f -mode wave packet through two identical small magnetic flux tubes ($R = 200$ km), embedded in a stratified atmosphere. We want to study the effect of separation d and incidence angle χ on the scattered wave. We have demonstrated that the horizontal compact pair of tubes ($d/R = 2$, $\chi = 0$) oscillate as a single tube when the incident wave is propagating, which gives a scattered wave amplitude of about twice that from a single tube. The scattered amplitude decreases with increasing d when d is about $\lambda/2\pi$ where λ is the wavelength of the incident wave packet. In this case the individual tubes start to oscillate separately in the manner of near-field scattering. When d is about twice of $\lambda/2\pi$, scattering from individual tubes reaches the far-field regime, giving rise to coherent scattering with an amplitude similar to the case of the compact pair of tubes. For perpendicular incidence ($\chi = \pi/2$), the tubes oscillate simultaneously with the incident wave packet. Moreover, simulations show that a compact cluster oscillates almost as a single individual small tube and acts more like a scattering object, while a loose cluster shows multiple-scattering in the near-field and the absorption is largest when d within the cluster is about $\lambda/2\pi$. This is the first step to understand the seismic response of a bundle of magnetic flux tubes in the context of sunspot and plage helioseismology.

Keywords: Helioseismology, direct modeling; Waves, magnetohydrodynamics; Sunspots; Plages, Magnetic fields

1. Introduction

One of the unsolved problems in solar physics concerns the magnetic structure of sunspots. Direct observations were unable to resolve this structure because of lack of sufficient spatial resolution, but also because of the hidden structure of the magnetic field below the visible solar surface. The simplest model is a

¹ Observatory of Algiers, CRAAG, Algiers, Algeria, email: k.daïffallah@craag.dz

monolithic magnetic flux tube which remains more or less homogeneous with increasing depth (Cowling, 1953).

The alternative model was proposed by Parker (1979) where the magnetic field of sunspot spreads into several discrete magnetic flux tubes below the visible surface of the Sun (cluster model). The debate between these two models is still relevant. However, Thomas, Cram, and Nye (1982) have suggested that indirect observations can answer the question about the structure of sunspot magnetic field. They argued that solar acoustic waves interact with sunspots, so that it would be possible to probe the structure beneath the surface by studying the observed wave field. The observations of Braun, Duvall, and LaBonte (1987, 1988) indicate that there is a significant absorption of f - and p -modes by sunspots. From this result, it is recognized as important to demonstrate that helioseismic waves interact differently with two distinct configurations of sunspot magnetic field. It was established that resonant absorption by fibril models of a sunspot can significantly increase the total acoustic energy absorption. Furthermore, fibril models produce a significant absorption across a wide range of plausible parameter values that can be adjusted unlike the monolithic model (Rosenthal, 1990). The first investigations about the interaction of acoustic waves with a bundle of magnetic flux tubes was limited to a statistical approach where a number of tubes are distributed uniformly or randomly in an infinite homogeneous atmosphere (Ryutov and Ryutova, 1976; Zweibel and Daepfen, 1989). These methods average the governing equations, which is less difficult mathematically, but relevant physical information will be lost.

Sunspots can also scatter waves. However, the theory of multiple scattering by magnetic flux tubes has been ignored in the past years due to the complexity of the problem. The multiple scattering was treated by using the formalism developed by Bogdan and Fox (1991). They studied the scattering of acoustic waves by a pair of uniform magnetic flux tubes for a series of separations in an unstratified atmosphere. Using the same formalism, Keppens, Bogdan, and Goossens (1994) studied wave interaction with a bundles of magnetic flux tubes in different geometrical configurations. This method finds the solution for each magnetic flux tube of the cluster considering both the incident acoustic wave and the scattered wave from all the other tubes. An important implication of these studies is that the cluster of tubes is more effective in absorption of acoustic waves than individual isolated tubes. For a single tube, the excitation is set by the incoming wave and it depends on the ratio of the tube-radius to the wavelength of the incoming wave (R/λ). However, in the flux tube bundle, the excitation must take into account multiple scattering of waves.

If the separation between the tubes within the cluster is not larger than the wavelength of the incoming wave, such that the tubes are in each others' near-field zones, the dominant excitation at each tube is provided by nearby neighbors rather than the contribution from the incident plane wave, leading to greatly enhanced scattered wave fields (multiple scattering).

When the tubes are far from the others ($d \gg \lambda$), the total scattering cross section is not different from the sum of individual flux-tube scattering cross section. Generally, the scattered fields interfere destructively in the far field (incoherent scattering).

For an intermediate separation, the scattering cross section of the bundle starts varying with the separation d , adding a coherent component to the cross section of the bundle (coherent scattering).

An important result is that the scattering behavior of a monolithic tube cannot be distinguished from that of a closely-packed fibril sunspot of the same magnetic flux.

The efforts mentioned above have been limited to the unstratified atmosphere, mainly because of the mathematical complexity that is introduced by the stratification. The analytical treatment is even more complicated for the scattering and absorption of waves by a cluster of magnetic flux tubes, while it is already quite complicated for the case of a single tube.

By using the same theoretical approach of Hanasoge *et al.* (2008) to describe the scattering matrix of a single thin-flux-tube, Hanasoge and Cally (2009) studied oscillation modes and scattering of a pair of flux tubes embedded in a gravitationally stratified atmosphere. They found that the strongest coupling is between the f -mode and the flux tubes where the dominant interaction distance is about half the horizontal surface wavelength of the incident waves ($\approx \pi/k$). They noticed also that the scattering coefficients attain large values at small flux tube separations. These results are similar to those of Bogdan and Fox (1991) and Keppens, Bogdan, and Goossens (1994) who suggested that a pair or a bundle of magnetic flux tubes can absorb waves quite effectively compared to a single monolithic tube.

We simulate in this study the propagation of a linear f -mode wave packet through a bundle of magnetic flux tubes in a three-dimensional polytropic stratified atmosphere. The aim is to distinguish between the monolithic and the cluster models of sunspots by studying the scattered waves and understand the interaction between waves and plage. The paper is organized as follows. In Section 2, we briefly describe the numerical code that we used and the set up of the simulations. In Section 3, we present the results of simulations of wave propagation through a pair of magnetic flux tubes which are arranged in parallel or perpendicular to the incident wave packet. In Sections 4 and 5, we compare the scattering of a monolithic magnetic flux tube with the scattering of a compact cluster of seven tubes, and a loose cluster of seven and nine tubes, respectively. Finally we conclude in Section 6.

2. Simulations

We used the SLiM code (Cameron, Gizon, and Daifallah, 2007) to solve the three-dimensional linearized wave equations in Cartesian geometry defined by the horizontal coordinates x and y , and the vertical coordinate z . We have periodic boundary conditions on the horizontal side walls of the simulation box. A pseudo-spectral scheme is implemented in the horizontal directions and a two-step Lax-Wendroff scheme in the vertical direction to evolve the horizontal Fourier modes.

As in Daifallah *et al.* (2011), the horizontal domain is $x \in [-20, 20]$ Mm and $y \in [-10, 10]$ Mm. The height range is from 0.2 Mm to 6 Mm below the solar

surface (z increases with depth). The initial condition is an f -mode wave packet propagating with a Gaussian envelope centered at the angular frequency 3 mHz with standard deviation of 1.18 mHz. At $t = t_0$, the wave packet is located at the left edge of the computational domain $x_0 = -20$ Mm, and it propagates from left to right in the x -direction. The background atmosphere is an enhanced polytropic atmosphere (Cally and Bogdan, 1997).

The initial individual magnetic flux tube is taken vertical in the z -direction and axisymmetric with a radial profile given by $B(r) = B_0 \exp(-r^4/R^4)$ where R is the tube radius, and $B_0 = 4820$ gauss (G). The flux tube is almost evacuated and it is superposed on the background atmosphere. The plasma- β value changes with depth according to the variation of the sound speed in the atmosphere. The sound speed is set to be equal to the Alfvén speed at a depth of 400 km.

The scattered wave field is constructed as the difference between the simulations with and without the flux tube.

3. f -Mode Interaction with Two Identical Magnetic Flux Tubes

To understand the interaction of a wave with an ensemble of magnetic flux tubes, it is useful to study the basic case where the bundle is composed of a pair of tubes aligned parallel or perpendicular (in the $x - y$ plane) to the direction of propagation of the incident wave packet. To simplify the interpretation of results, we consider that all individual tubes are identical with radius $R = 200$ km. Figure 1 shows how the pair of flux tubes are positioned in horizontal or perpendicular configuration. The reference tube in black contour is situated at the position $(-7, 0)$. The white contours represent successive positions of the second tube.

We define χ as the angle between the direction of propagation of the incident wave packet and the line connecting the reference tube to the second tube. The second tube located on the right-hand-side of the reference tube in Figure 1 corresponds to $\chi = 0$. The tube located in the y -direction corresponds to $\chi = \pi/2$. The separation between the successive centers of the pair of tubes varies as $d = 2R, 3R, 4R, 5R$, and $10R$ which correspond to $d = 0.08\lambda, 0.12\lambda, 0.16\lambda, 0.2\lambda$, and 0.4λ , respectively, where $\lambda \approx 4.85$ Mm is the wavelength of the f -mode ($2\pi g/\omega^2$) for the wave packet centered at 3 mHz.

We have analyzed the velocity V_z at point B(-14.0) situated in the scattered wave field on the left of the reference tube. The scattering there is more interesting to analyze because it shows oscillations of the magnetic flux tube without contribution from the incident wave packet.

The scattering process is predominantly restricted to $f - f$ mode, while the $f - p$ mode conversions are very weak (Hanasoge *et al.*, 2008; Daiffallah *et al.*, 2011). ■

3.1. A Pair of Magnetic Flux Tubes with $\chi = 0$

In this subsection, we investigate the f -mode interaction with a pair of magnetic flux tubes aligned in the x -direction ($\chi = 0$). Figure 2 shows the time variations of the vertical velocity V_z measured at point B as a function of the separation

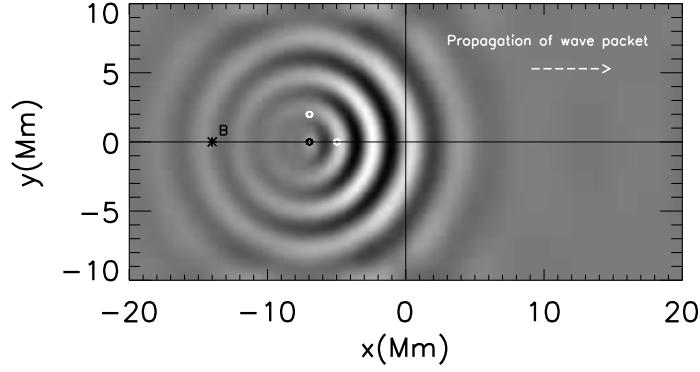


Figure 1. Scattered wave field due to the reference tube (black contour) and the second tube (white contour). The second tube to the right and in the y -direction corresponds to the angle $\chi = 0$ and $\chi = \pi/2$, respectively. The separation distance d between the reference tube and the second tube changes from $d = 0.08\lambda$ to $d = 0.4\lambda$; $\lambda \approx 4.85$ Mm is the wavelength of the f -mode. The unit tube has a radius $R = 200$ km. The scattered component V_z is measured at point B $(-14, 0)$ for all simulations. The reference tube is situated at the position $(-7, 0)$.

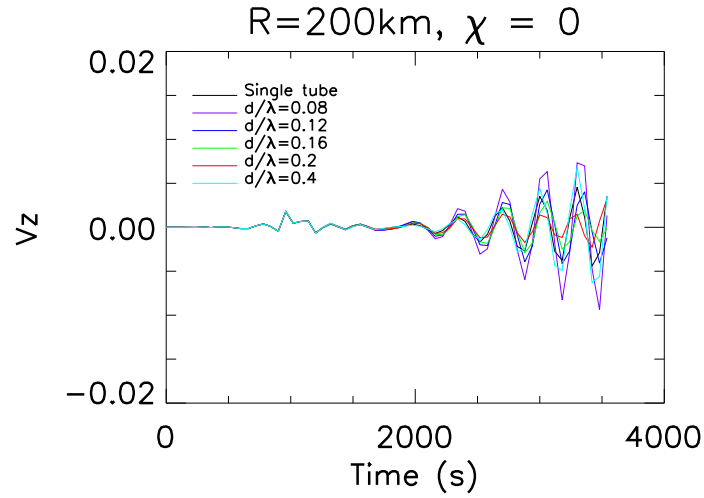


Figure 2. Scattered vertical velocity (V_z) as a function of time, measured at point B for a pair of magnetic flux tubes ($\chi = 0$). Point B is indicated in Figure 1. The color curves are for different separation distances d between the reference and the second tubes.

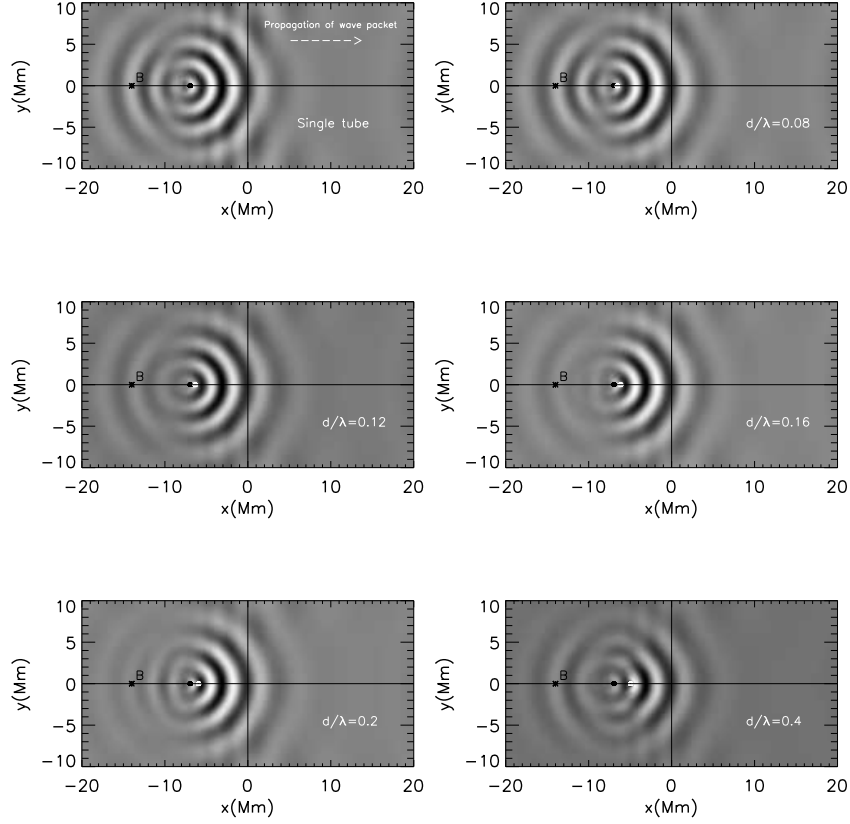


Figure 3. Scattered wave field of V_z at $t = 3300$ s for a pair of magnetic tubes with $\chi = 0$. The reference and the second tubes are represented with black and white contours, respectively. The top left figure corresponds to the scattering of a single tube ($R = 200$ km). The following figures show the variation in scattering with the distance between the two tubes. The separation varies as $d/\lambda = 0.08, 0.12, 0.16, 0.2$, and 0.4 , respectively.

distance d between the pair of flux tubes. The black curve shows the scattering from a monolithic flux tube of 200 km radius.

First, we note that the scattering curves of different pairs measured at point B are slightly out of phase, which means that the motion of the pair of tubes changes with the separation d . The curves show that the compact pair ($d/\lambda = 0.08$) has the largest scattering amplitude compared to the others. This amplitude is approximatively the scattering amplitude of a single tube of 400 km radius ($2R$).

The scattering amplitude for $d/\lambda = 0.4$ is also large as the case of $d/\lambda = 0.08$. The curves corresponding to $d/\lambda = 0.12, 0.16$, and 0.2 are below the curve for the compact pair $d/\lambda = 0.08$.

Figure 3 shows the scattered wave field due to a pair of flux tubes with $\chi = 0$ at $t = 3300$ s. We can see that the wave field to the left is totally influenced by the

tube oscillations. For a separation of $d/\lambda = 0.08$, the scattered wave field to the left (dipole oscillations) is very similar to that of a single tube, which indicates a strong coupling between the two tubes. For the other separations, the pattern of the near-field scattering changes according to the mutual interaction between the tubes. For $d/\lambda = 0.4$, we begin to clearly distinguish the waves scattered by the tubes separately.

It is interesting to plot the x -displacement of the tube axis as a function of depth z to see the tube oscillations. Figure 4 shows snapshots of the x -displacement at $t = 2100$ s. The solid curves are for the pair of tubes. The dashed curve shows the oscillation of the reference tube ($R = 200$ km) when it is single. The first snapshot shows that the displacement amplitude of the reference tube is larger than the displacement amplitude of this tube when it is single. This demonstrates the effect of the second tube and consequently the increase in the amplitude when the pair is compact. Because of the very close separation, we see that the oscillations of the two tubes are substantially in phase relative to the other cases with larger values of d/λ . The last snapshot for $d/\lambda = 0.4$ shows that the x -displacement of the tubes is completely in the opposite directions.

3.1.1. Interference Effect between the Two Tubes with $\chi = 0$

In Figure 3, the scattered wave field generated by the pair of tubes tends to obscure the mutual interference between the two tubes. This interference is very important to understand the degree of influence of one tube to the other depending on the separation distance d/λ . We have applied a method to extract the total scattered field to see only the field due to interference. Figure 5 illustrates this procedure.

This method gives rise to some noisy behavior of the wave field to the right of the tubes, but this will not disturb our analysis since we are interested in the wave field to the left of the tubes. Figure 6 shows the interference field of velocity V_z for pairs with separation $d = 0.12\lambda, 0.2\lambda$, and 0.4λ , respectively. In these snapshots, waves scattered by the reference tube to the left are the result of waves scattered by the second tube and vice versa. In the case of $d/\lambda = 0.12$, the tubes are so close that their oscillations are almost in phase. As a result, the interference effect produced by the tubes remains the same during the propagation of the incident wave, which explains the symmetrical pattern of the waves scattered by the tubes on both sides (left and right wave fields). The mutual interference between the tubes starts to be different as the separation d increases. In the case of $d/\lambda = 0.4$, the interference field is no more symmetrical since the tubes oscillate differently.

We have found that the amplitude of mutual excitation of tubes in the x -direction is minimum for small separation d and increases with d . This is in good agreement with the previous results where the amplitude of the waves scattered by the pair of tubes decreases with increasing d when $d \leq 0.2\lambda$. In this case, the pair of tubes oscillate almost as a single tube leaving only a small energy to the oscillations of the individual tubes, which explains maximum scattering and low interference for the case of $d = 0.08\lambda$. Thus, the change in the scattered near-field to the left of the tubes in Figure 3 for $0.12\lambda \leq d \leq 0.2\lambda$ is caused by

Propagation of wave packet

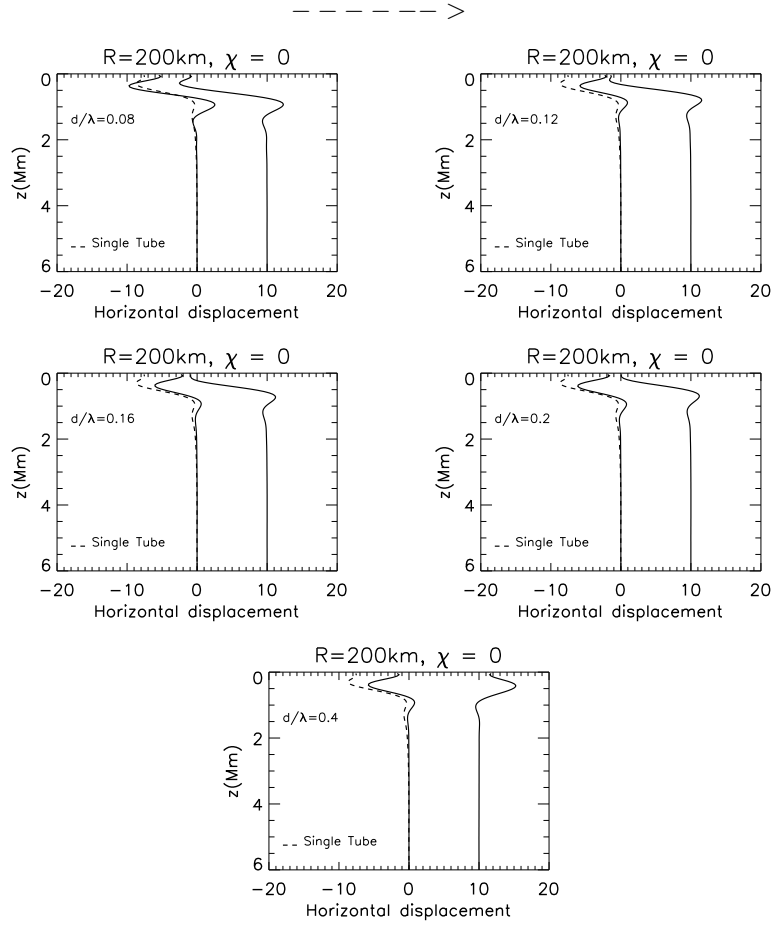


Figure 4. Displacement of the two tube axes in arbitrary units in the x -direction (solide lines) as a function of depth z . The dashed curves show the x -displacement of the reference tube when it is single ($R = 200$ km). The solid curves are snapshots at $t = 2100$ s after the start of the simulation and show oscillations of a pair of tubes ($\chi = 0$) for various values of the separation d .

the small oscillations of the tubes. This corresponds to the multiple scattering regime.

For larger separation $d > 0.2\lambda$, the individual tubes start to oscillate more effectively with respect to the collective oscillation of the pair of tubes. Therefore, a part of the power of the incident wave will supply these oscillations. Consequently, the mutual interaction between the tubes increases. However, the scattering measured at point B for $d = 0.4\lambda$ (Figure 2) increases again compared to the case of $d = 0.2\lambda$. In fact, the different phases of scattered waves by the

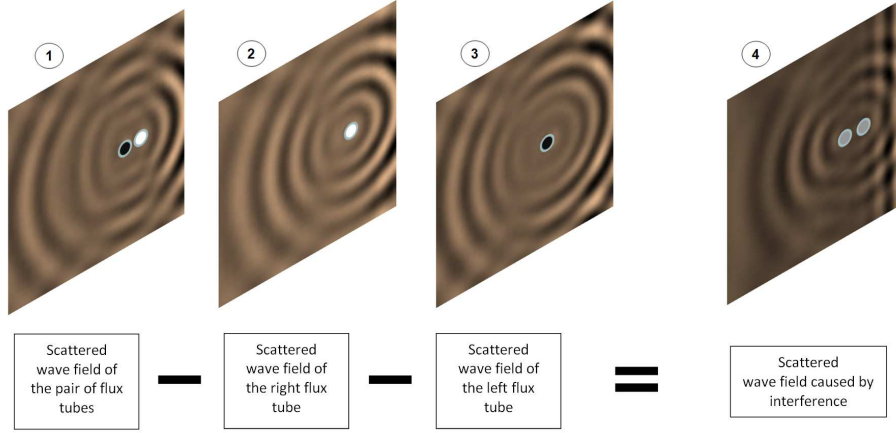


Figure 5. The interference wave field (4) is obtained by the subtraction from the image of the scattered wave field of the two tubes (1) the image of the scattered wave field of the reference tube (2) and the second tube (3), respectively, when they are single. The resulting image corresponds to the effect of mutual interference of the waves from the two tubes only.

Propagation of wave packet

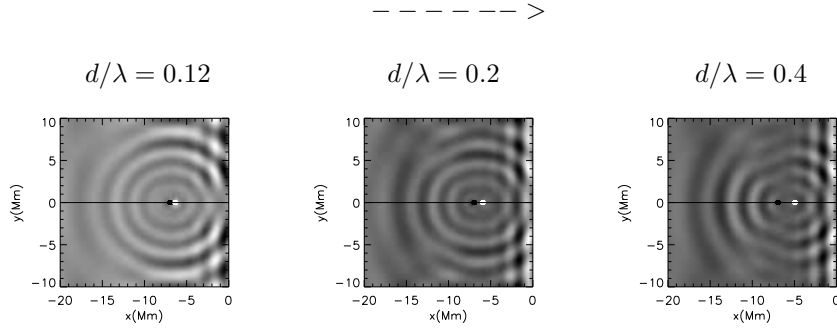


Figure 6. Snapshots at $t = 4200$ s of the vertical component V_z showing the interference field of the two tubes ($\chi = 0$) for various values of the separation d . From left to right $d/\lambda = 0.12, 0.2$, and 0.4 , respectively.

tubes interact and interfere constructively in the far-field giving rise to a coherent scattering regime.

3.2. A Pair of Magnetic Flux Tubes with $\chi = \pi/2$

We simulate in this subsection the interaction of an *f*-mode wave packet with a pair of magnetic flux tubes aligned in the y -direction ($\chi = \pi/2$) (Figure 1).

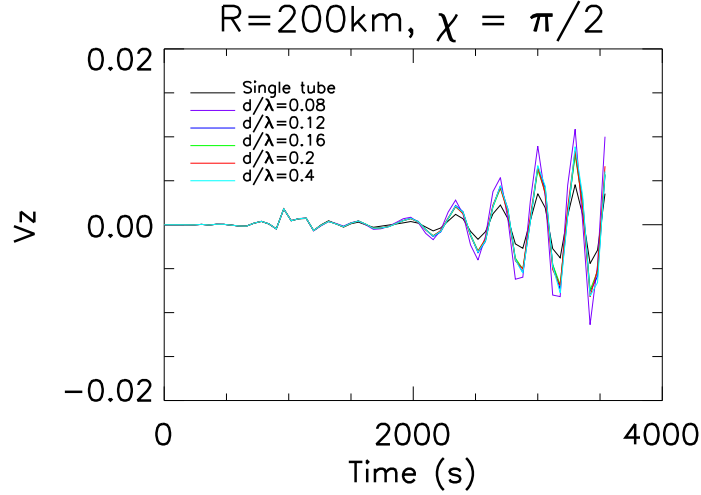


Figure 7. Scattered vertical velocity as a function of time measured at point B for a pair of magnetic flux tubes ($\chi = \pi/2$). Point B is indicated in Figure 1. The color curves are for different separation distances d between the reference and the second tubes.

Figure 7 shows the time variations of the scattered vertical velocity V_z measured at point B for different separation distances d .

The incident wave arrives and excites simultaneously the pair of the tubes. The consequence is that the different curves are perfectly in phase. Figure 7 shows that the scattered V_z is maximum for compact tubes ($d/\lambda = 0.08$) as in the case of $\chi = 0$. We can approximate this configuration of two compact tubes aligned in the y -direction to a single tube of 400 km radius ($2R$), which explains the increase in the scattered wave amplitude. However, we note that this amplitude exceeds that of the case $\chi = 0$, which implies the contribution of both tubes in the scattering measured at point B unlike the case of $\chi = 0$.

The scattered wave field for $d/\lambda = 0.08, 0.12, 0.16$, and 0.2 shows similarity with the scattering from a single tube. In the case of $d/\lambda = 0.4$, the individual contribution of each tube starts to appear in the near-wave field, but the tubes stay synchronized according to Figure 7.

The case of $\chi = \pi/2$ is similar to the case where the incident wave propagates in the z -direction through a pair of flux tubes. In both cases, the tubes are excited and oscillate simultaneously.

4. f -Mode Interaction with a Compact Cluster of Seven Flux Tubes

In this section, we study the interaction of an f -mode wave packet with a cluster of seven identical magnetic flux tubes in a hexagonal close-packed configuration. This is the simplest “realistic” structure that can be built to simulate the cluster model of sunspots.

The cluster model can be a good approximation to simulate solar plage regions which are composed of an ensemble of compactly packed thin flux tubes. It is

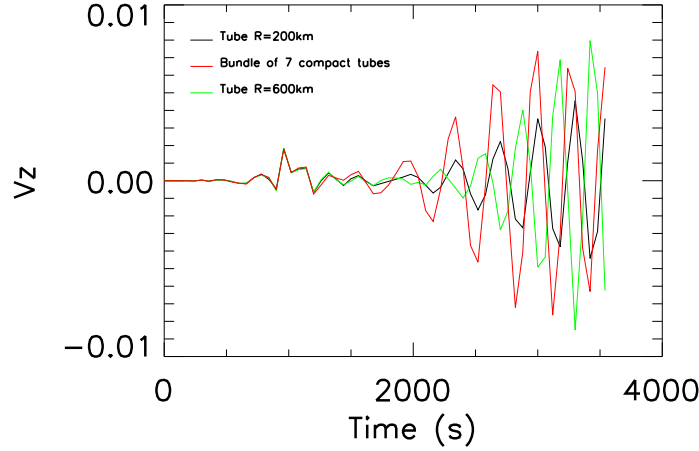


Figure 8. Scattered vertical velocity as a function of time measured at point B. The black and the green curves are for monolithic flux tubes with radii of 200 km and 600 km, respectively, situated at the same position of the central tube in the cluster. The red curve is the scattering from a compact cluster of seven tubes.

important to understand wave absorption and scattering by the plage in relation to the energy transmitted to the corona (Hanasoge and Cally, 2009).

Figure 8 shows the variation of the scattered component V_z versus time at point B for a single monolithic tube of 200 km radius (black curve), a compact cluster of seven tubes (red curve), and a single tube of 600 km radius which is the monolithic equivalent of the compact cluster (green curve).

First, we can observe that the cluster yields a large amplitude of scattered waves compared to the 200 km single tube. This amplitude is almost the same as the amplitude due to the monolithic equivalent tube of 600 km radius.

The curve of the compact cluster shows an interesting behaviour. The cluster seems to oscillate almost like a tube of 200 km radius than like a tube of 600 km radius. The scattered wave fields of the compact cluster and the single tube of 200 km radius show almost an identical pattern too. This trend may be attributed to the forcing of the collective oscillations in the compact cluster dominated by the kink mode ($m = \pm 1$) in the individual flux tubes of 200 km radius, whereas the monolithic tube of 600 km radius oscillates with a mixture of sausage ($m = 0$) and kink modes (Bogdan *et al.*, 1996; Daifallah *et al.*, 2011).

5. *f*-Mode Interaction with a Loose Cluster

In this section, we study the scattering from a loose cluster composed of seven and nine identical magnetic flux tubes ($R = 200$ km). The distance between the central tube to the other tubes is $d/\lambda = 0.2$ for both clusters.

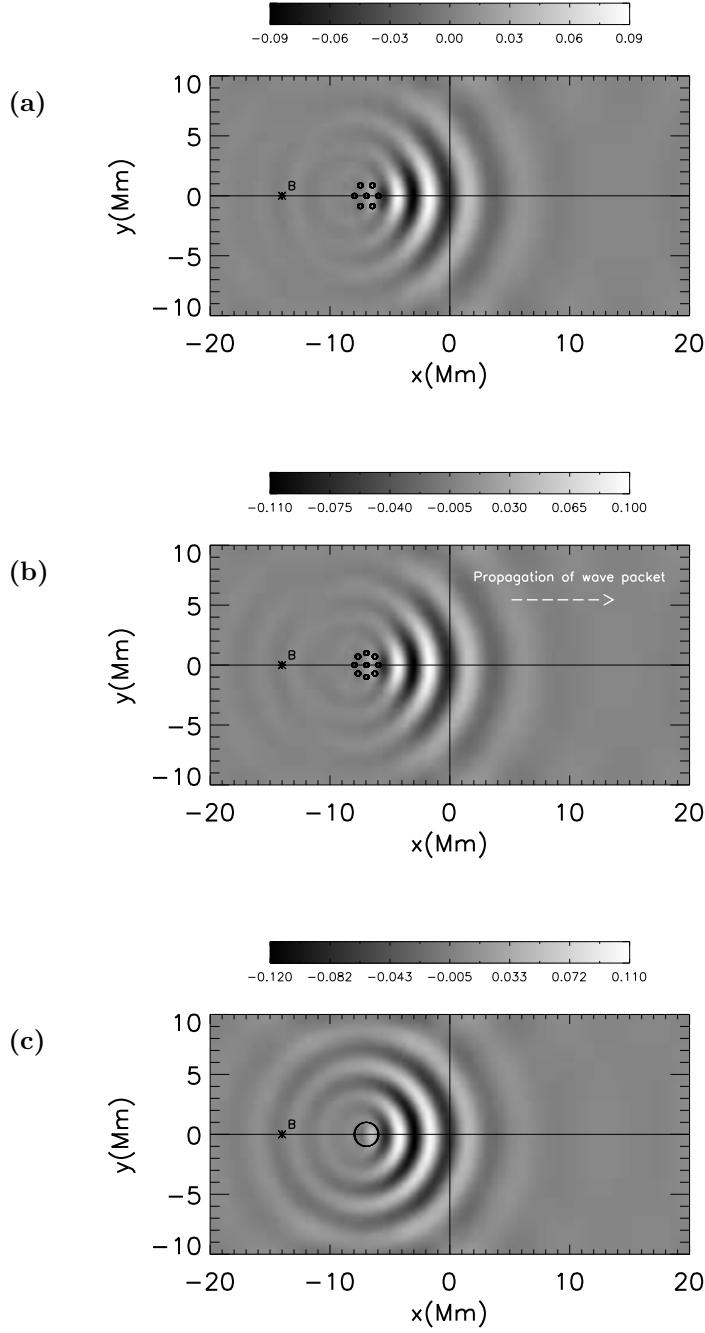


Figure 9. (a) A snapshot at $t = 3300$ s of the scattered wave field (V_z) of a loose cluster of seven identical magnetic flux tubes of 200 km radius. The distance from the central tube to the others is $d = 0.2\lambda$. (b) The same as (a) but for a loose cluster of nine identical tubes of 200 km radius with separation $d = 0.2\lambda$. (c) The same as (a) but for a monolithic tube whose radius $R = 1$ Mm is the average radius of both clusters in (a) and (b).

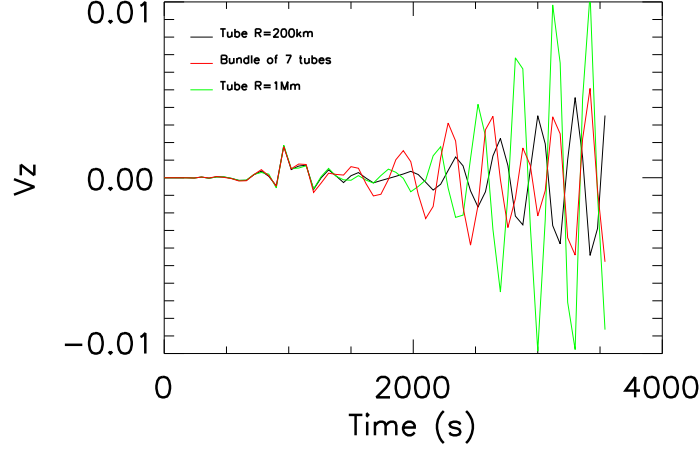


Figure 10. Scattered vertical velocity as a function of time measured at point B. The black and the green curves are for monolithic flux tubes with radii of 200 km and 1 Mm respectively, situated at the same position of the central tube in the cluster. The red curve is the scattering from a loose cluster of seven tubes (Figure 9(a)).

Figure 9(a)-9(c) shows the scattered wave fields (V_z) of a seven-tube cluster, a nine-tube cluster, and a single tube of 1 Mm radius which is approximately the equivalent monolithic tube to the cases of Figures 9(a) and 9(b).

5.1. Loose Cluster of Seven Flux Tubes

We have done this case to compare the scattering from a compact cluster to the scattering from the same cluster when it is loosely distributed.

An important change can be seen in the near-field scattered wave to the left of the loose cluster (Figure 9(a)) compared to the case of the monolithic tube. This indicates the contribution of waves scattered by individual tubes while the compact cluster shows no multiple scattering in the near-field.

Figure 10 shows a plot of the scattered vertical velocity V_z measured at point B as a function of time for the loose cluster of seven tubes, and single tubes with radii of 200 km and 1 Mm. For separation distance $d/\lambda = 0.2$, the individual tubes start to oscillate differently compared to the collective oscillations of tubes in the compact cluster; as a consequence, the oscillations of 200 km tube and the loose cluster in Figure 10 are no longer in phase.

We found that the amplitude of scattered waves from the loose cluster is smaller compared to that from the compact cluster in Figure 8. According to the results of Section 3, the spacing within the loose cluster ($d/\lambda = 0.2$ from the central tube) supports only a small-amplitude oscillation of individual flux tubes which scatter waves to the near-field (multiple scattering). Consequently, the scattering measured in the far-field will be reduced compared to that from the compact cluster since some of the incident wave energy is converted to tube

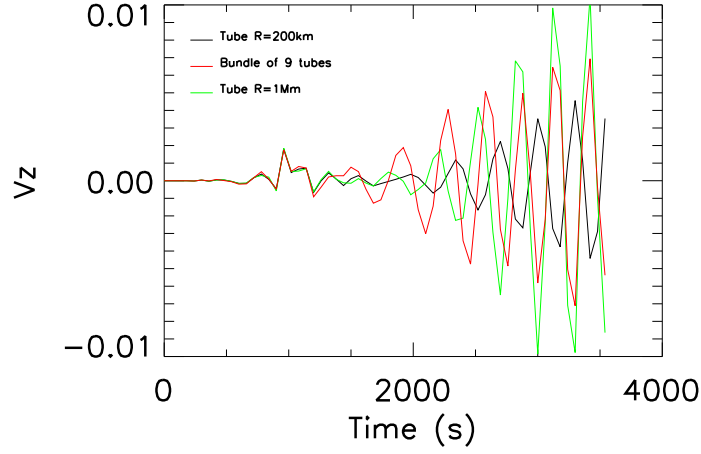


Figure 11. A plot of the scattered vertical velocity as a function of time measured at point B. The black and the green curves are for monolithic flux tubes of 200 km and 1 Mm radius, respectively, situated at the same position of the central tube in the cluster. The red curve is the scattering from a loose cluster of nine tubes (Figure 9(b)).

oscillations. In this case, if we interpret the reduction in the far-field scattering as an enhancement of absorption of waves by the loose cluster model, then a loose cluster can be more absorbent (scatters less) than a compact cluster when $0.12\lambda < d \leq 0.2\lambda$. However, when $0.2\lambda < d \leq 0.4\lambda$, the loose cluster should be more absorbent since oscillations of individual tubes are more efficient than in the previous case. However, coherent scattering to the far-field increases the amplitude again, in this case, measuring scattering in the far-field to evaluate absorption of waves is no longer valid.

5.2. Loose Cluster of Nine Flux Tubes

As in the previous case, multiple scattering to the near-field can be seen in the scattered wave field to the left of the loose cluster (Figure 9(b)). In Figure 11 are shown the curves of scattered vertical velocity V_z measured at point B as a function of time. From Sections 3 and 4, we know that the maximum scattering amplitude that can be reached by the cluster is the amplitude of the equivalent monolithic tube. From these results, it is clear that the reduction in amplitude of the loose cluster in Figure 11 is a signature of absorption of waves by individual flux tubes giving rise to the near-field scattering. We note, however, that this amplitude is larger than the amplitude of the scattered waves from the seven-tube loose cluster. This result means that a cluster in the multiple scattering regime scatters waves more to the far-field than a less dense cluster with the same size.

If we increase the density of the same cluster by taking $d/\lambda = 0.16$, the amplitude of the scattered waves in the far-field will increase too, approaching that of the equivalent tube of 1 Mm radius.

6. Conclusions

While sunspots are easily visible, finding their structure beneath the solar surface is not an easy task. Motivated by the problem of subsurface magnetic structure of sunspots, we investigate numerically the wave propagation through a cluster model of magnetic flux tubes. The goal is to distinguish helioseismically between this model and the monolithic model of sunspots by observing the scattered wave field.

The multiple flux tube model is a good model for plage as well. The attenuation of the waves in the plage regions is enhanced and this type of simulation provides a good way of understanding that.

In the first part of this study, we have simulated the interaction between an *f*-mode wave packet and a pair of small identical magnetic flux tubes of radius $R = 200$ km positioned along (*x*-direction) or perpendicular (*y*-direction) to the direction of propagation of the incoming waves.

For the pair aligned in the *x*-direction, when the distance between the tubes d is less than $\lambda/2\pi$ (λ is the wavelength of the incident wave packet), the pair of tubes oscillate as a single tube. The result is a maximum amplitude of scattering measured at the far-field. The amplitude of the scattered wave from the compact pair is about the same as that from a single tube of $2R$ radius.

When separation d is about $\lambda/2\pi$, the individual tubes start to oscillate and scatter waves to the near-field (multiple scattering regime) taking a part of the energy of the scattered wave. Then, the amplitude of the scattered wave decreases. When d is about twice of $\lambda/2\pi$, oscillations from individual tubes increase and reach the level of the far-field scattering, giving rise to a coherent scattering. The amplitude increases again to about that from the compact pair of tubes (coherent scattering regime).

For the pair of flux tubes aligned in the *y*-direction, the tubes oscillate simultaneously with the incoming waves.

In order to obtain more realistic models for sunspots and plage, we have investigated the propagation of waves through a cluster of small identical magnetic flux tubes of 200 km radius. We have studied two cases, one is a compact cluster and the other is a loose cluster. The compact cluster seems to oscillate more like a single tube of 200 km radius than like the monolithic equivalent tube, while the scattering behavior of the loose cluster shows multiple-scattering from the individual tubes in the near-field. However, the scattered amplitude of the compact cluster measured in the far-field is almost the same as the scattered amplitude of the monolithic equivalent tube.

We have demonstrated that a loose cluster in the multiple scattering regime is more efficient in absorption of waves than a compact cluster or the equivalent monolithic tube of both kinds of clusters. It is reasonable to infer that less is the density of tubes within a cluster, more is the absorption of waves by individual flux tubes and less is the scattering to the far-field. However, it is unclear how to evaluate the absorption of waves by a cluster in the coherent scattering regime since scattering is enhanced in the far-field.

Notice that we are discussing interaction of surface gravity waves (*f*-mode) with small radius flux tubes. In this context, the scattering *f*-*f* modes will be

the predominant process compared to the absorption and propagation of waves in the z -direction. Therefore, it will be no surprising to find more absorption of waves for p -mode interaction with magnetic flux tubes and clusters.

Future investigations require more simulations using different sizes of magnetic flux tubes, various geometrical configurations, p -modes as an incident wave packet. More spatial and temporal resolutions are required to study the near-field phenomena and the interaction among tubes within the cluster.

References

- Bogdan, T.J., Fox, D.C.: 1991, Multiple scattering of acoustic waves by a pair of uniformly magnetized flux tubes. *Astrophys. J.* **379**, 758–775. doi:10.1086/170552.
- Bogdan, T.J., Hindman, B.W., Cally, P.S., Charbonneau, P.: 1996, Absorption of p -modes by slender magnetic flux tubes and p -mode lifetimes. *Astrophys. J.* **465**, 406–424. doi:10.1086/177429.
- Braun, D.C., Duvall, T.L., Jr., LaBonte, B.J.: 1987, Acoustic absorption by sunspots. *Astrophys. J. Lett.* **319**, L27–L31. doi:10.1086/184949.
- Braun, D.C., Duvall, T.L., Jr., LaBonte, B.J.: 1988, The absorption of high-degree p -mode oscillations in and around sunspots. *Astrophys. J.* **335**, 1015–1025. doi:10.1086/166988.
- Cally, P.S., Bogdan, T.J.: 1997, Simulation of f - and p -mode interactions with a stratified magnetic field concentration. *Astrophys. J. Lett.* **486**, L67–L70. doi:10.1086/310833.
- Cameron, R., Gizon, L., Daifallah, K.: 2007, SLiM: A code for the simulation of wave propagation through an inhomogeneous, magnetised solar atmosphere. *Astron. Nachr.* **328**, 313–318. doi:10.1002/asna.200610736.
- Cowling, T.G.: 1953, Solar electrodynamics. In: Kuiper, G.P. (ed.) *The Sun*, University of Chicago Press, Chicago, 532–591.
- Daifallah, K., Abdelatif, T., Bendib, A., Cameron, R., Gizon, L.: 2011, 3D Numerical simulations of f -mode propagation through magnetic flux tubes. *Solar Phys.* **268**, 309–320. doi:10.1007/s11207-010-9666-5.
- Hanasoge, S.M., Cally, P.S.: 2009, Multiple scattering of waves by a pair of gravitationally stratified flux tubes. *Astrophys. J.* **697**, 651–659. doi:10.1088/0004-637X/697/1/651.
- Hanasoge, S.M., Birch, A.C., Bogdan, T.J., Gizon, L.: 2008, f -mode interactions with thin flux tubes: The scattering matrix. *Astrophys. J.* **680**, 774–780. doi:10.1086/587455.
- Keppens, R., Bogdan, T.J., Goossens, M.: 1994, Multiple scattering and resonant absorption of p -modes by fibril sunspots. *Astrophys. J.* **436**, 372–389. doi:10.1086/174912.
- Parker, E.N.: 1979, Sunspots and the physics of magnetic flux tubes. I - The general nature of the sunspot. *Astrophys. J.* **230**, 905–912. doi:10.1086/157150.
- Rosenthal, C.S.: 1990, Absorption of acoustic waves in monolithic and fibril sunspot models. *Solar Phys.* **130**, 313–335. doi:10.1007/BF00156796.
- Ryutov, D.A., Ryutova, M.P.: 1976, Sound oscillations in a plasma with "magnetic filaments". *Soviet Phys. JETP* **43**, 491–497.
- Thomas, J.H., Cram, L.E., Nye, A.H.: 1982, Five-minute oscillations as a subsurface probe of sunspot structure. *Nature* **297**, 485–487. doi:10.1038/297485a0.
- Zweibel, E.G., Daeppen, W.: 1989, Effects of magnetic fibrils on solar oscillation frequencies - Mean field theory. *Astrophys. J.* **343**, 994–1003. doi:10.1086/167768.